Conditional mixing statistics in a self-similar scalar mixing layer

Stephen M. de Bruyn Kops
Department of Mechanical and Industrial Engineering, University of Massachusetts Amherst, Amherst, Massachusetts 01003

Mikael Mortensen
Department of Chemical Engineering and Environmental Science, Chalmers University of Technology, Gothenburg 412 96, Sweden

(Received 22 March 2005; accepted 5 August 2005; published online 26 September 2005)

Conditional scalar mixing statistics from a three-dimensional direct numerical simulation (DNS) of a scalar mixing layer are presented in the context of modeling nonpremixed turbulent combustion. The simulation is closely matched to a particular laboratory experiment but with slight adjustments so that the simulated flow is very nearly self-similar. All statistics commonly used in mixing models are presented, along with comparisons to models and laboratory data where available. A model for the conditional scalar dissipation rate (CSD), recently introduced by Mortensen ["Consistent modeling of scalar mixing for presumed multiple parameter probability density functions," Phys. Fluids **17**, 018106 (2005)], is tested against the data set, as is a Lagrangian stochastic trajectory technique recently published by Sawford ["Conditional scalar mixing statistics in homogenous isotropic turbulence," New J. Phys. **6**, 1 (2004)]. It is concluded that (i) the DNS data set provides an excellent, high-resolution description of the scalar mixing layer that can be used for developing and verifying models for scalar mixing; (ii) the self-consistent CSD model of Mortensen is necessary for consistent implementations of the conditional moment closure, but for the current flow it gives only small adjustments to the more commonly adopted model of Girimaji ["On the modeling of scalar diffusion in isotropic turbulence," Phys. Fluids A **4**, 2529 (1992)]; and (iii) Sawford's Lagrangian technique very closely predicts the DNS results. © *2005 American Institute of Physics*. [DOI: 10.1063/1.2055467]

I. INTRODUCTION

For modeling non-premixed turbulent combustion, understanding mixing of passive scalars in canonical flow configurations continues to be of significant importance.[1] Despite the fact that many basic flows have been studied extensively, there is a need for more data in part because much of the literature pre-dates current modeling approaches and thus does not report certain statistics that are now of interest. For instance, Sawford[2] notes that of all the published data on scalar mixing layers, to his knowledge only that of Li and Bilger[3] includes (a partial set of) the conditional statistics he needs for model testing. In this paper, mixing statistics from previously published[4] high-resolution direct numerical simulations (DNSs) of a scalar mixing layer are presented in the context of current modeling approaches for non-premixed turbulent combustion.

The scalar, or thermal, mixing layer, which involves the mixing of two scalar streams in homogeneous isotropic turbulence, is one of the most basic flow configurations involving the transport of passive scalars. As such, it has been studied extensively using laboratory, numerical, and theoretical approaches.[3–10] Among the interesting attributes of the flow configuration is that the equations of motion allow for a self-similar solution in the limit of infinite Peclet number. Thus far, it has proven difficult to realize the self-similar configuration in a wind tunnel, in part because of the mechanical challenge of initiating the scalar field to have the same virtual origin as the velocity field, and in part because of finite Reynolds number effects. Using high-resolution DNS, de Bruyn Kops and Riley[4] generated a data set that is closely matched to the laboratory experiments of Ma and Warhaft,[8] except that the virtual origins of the scalar and velocity fields are aligned. In this flow simulation, only a very slight deviation from self-similarity exists due to the effects of molecular diffusion. The data set provides a description of the flow as a function of three spatial dimensions plus time, so that arbitrary quantities of importance in modeling nonpremixed combustion and other phenomena can be computed.

The most common approach to predicting turbulence using numerical simulations is to Reynolds average or, in the case of large eddy simulations, filter the governing transport equations and then model terms that involve products of the fluctuating quantities. In combustion simulations, applying this technique to the reacting scalars has proven to be problematic. An alternative approach to Reynolds averaging is to begin with the evolution equation for the joint probability density function (JPDF) of the velocity and scalar, which can be derived exactly from the momentum and scalar conservation equations.[11]

Solving the eight-dimensional JPDF equation is a challenging numerical problem that traditionally has been done using Lagrangian stochastic methods. More commonly, combustion research related to PDF methods has been focused on the transport equation for the probability density of the sca-

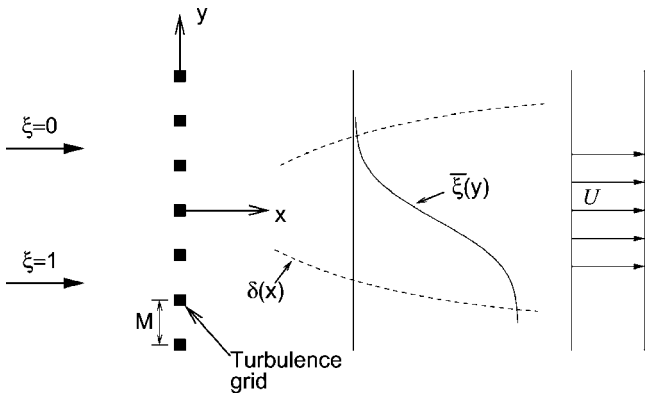

FIG. 1. Schematic of a scalar mixing layer.

lar, which can be derived by integrating the JPDF equation over velocity. Taking the scalar to be the mixture fraction, ξ, under the assumptions of constant diffusivity κ and uniform density, the equation for the PDF of ξ, p_ξ, can then be written[12]

$$\frac{\partial p_\xi}{\partial t} + \nabla \cdot (\langle \mathbf{v} | \eta \rangle p_\xi) = -\frac{1}{2}\frac{\partial^2 (\langle \chi | \eta \rangle p_\xi)}{\partial \eta^2} + \kappa \nabla^2 p_\xi. \tag{1}$$

Here $\langle \mathbf{v} | \eta \rangle = \langle \mathbf{v} | \xi = \eta \rangle$ is the mean velocity conditional on $\xi = \eta$ (η is the sample space variable for ξ) and $\langle \chi | \eta \rangle$ is the conditional scalar dissipation rate.

It is apparent that to model (1), data for $p_\xi, \langle \mathbf{v} | \eta \rangle$, and $\langle \chi | \eta \rangle$ are of interest. Some researchers are interested in the conditional scalar diffusion rate since the right-hand side of (1) can be rewritten in terms of this quantity. In addition, other quantities, including the unconditionally averaged scalar dissipation rate, the scalar flux, the turbulent diffusivity, and the ratio of the mixing and turbulent time scales are often of interest when developing mixing models. In this paper, we present data for all these quantities from the direct numerical simulations and compare with predictions of models in common use, results from a Lagrangian stochastic trajectory simulation,[2] and laboratory data where available. Before we do this, though, we provide an overview of the simulations in the next section.

II. DIRECT NUMERICAL SIMULATIONS

A schematic of a scalar mixing layer is shown in Fig. 1. It is simulated in three dimensions using a numerical method that is discussed in detail by de Bruyn Kops and Riley.[4,13] Briefly, a pseudo-spectral method is used to advance the Navier-Stokes equations in time using a third-order fractional step method for time stepping. Periodic boundary conditions are used in the streamwise (x) and spanwise (z) directions. Periodic boundary conditions are also used in the direction of the scalar gradient (y) so that two realizations of the mixing layer can be run simultaneously. The numerical domain size is $512 \times 1024 \times 512$ grid points ($x \times y \times z$). The somewhat involved process of initializing the scalar so as to have the same virtual origin as the velocity field is discussed in Ref. 4. Of importance when discussing certain quantities later in this paper is the orientation of the layer with respect to the y-direction: $\xi \to 1$ as $y \to -\infty$ and $\xi \to 0$ as $y \to \infty$.

TABLE I. Gross properties of the laboratory scalar mixing layer velocity fields. The velocity data of Bilger *et al.* (Ref. 10) have been corrected per Ref. 14.

	LaRue *et al.* (1981)	Ma and Warhaft (1986)	Bilger *et al.* (1991)
x/M		100	12
U (cm/s)	780	620	50
u/U		0.014	0.080
v/U		0.012	0.040
$\bar{\epsilon}$ (cm^2/s^3)		361	2.40
M (cm)	4	2.50	32
L (cm)		1.66	17.0
λ (cm)		0.620	2.708
η_k (cm)		0.0549	0.324
$\mathrm{Re}_M = UM/\nu$	21010	9394	11700
$\mathrm{Re}_L = u_{\mathrm{rms}} L/\nu$		84.8	455
$\mathrm{Re}_\lambda = u_{\mathrm{rms}} \lambda/\nu$		32.7	72.5
Test section x/M	21-67	62.4-132.4	12-21

The simulations are initialized to match the laboratory experiment of Ma and Warhaft,[8] the conditions for which are given in Table I. Also shown in the table are the conditions for other experiments that are referenced in this paper. The symbols in the table are: U (mean velocity in the x-direction), u, v (turbulent velocity fluctuations in the x-, y-directions), $\bar{\epsilon}$ (dissipation rate of turbulence kinetic energy), M (pitch of the wire mesh used to generate the turbulence), L (velocity longitudinal integral length scale), λ (Taylor microscale), η (Kolmogorov length scale), and u_{rms} (rms turbulent velocity fluctuations). In this paper, we discuss results of temporal simulations in terms of wind tunnel coordinates since many researchers find them more familiar. The numerical domain is scaled to the dimensions $25.1 \times 50.3 \times 25.1$ cm^3 and Taylor's hypothesis is invoked to convert between simulation time and downstream location. As a result, all quantities from the simulations can be compared directly with the corresponding values from the experiments of Ma and Warhaft.

Taking into consideration all of the statistical quantities presented in Ref. 4, it can be concluded that the simulated flow is very nearly self-similar and free from the effects of the boundary conditions for x/M values between 50 and 150. The only relevant spatial coordinate is the cross-steam location scaled by the characteristic width of the mean scalar profile; i.e., y/δ. Here, δ is defined as the length from the center of the mixing layer to the point where the mean mixture fraction is 0.92. As a consequence of there being no dependence on downstream location, the data from multiple x/M locations can be aggregated to improve the certainty of statistics. In this paper, data from 18 downstream locations between $x/M = 50$ and $x/M = 150$, for a total of 4.8 billion data points, are used for the computation of all statistics reported in this paper unless noted otherwise.

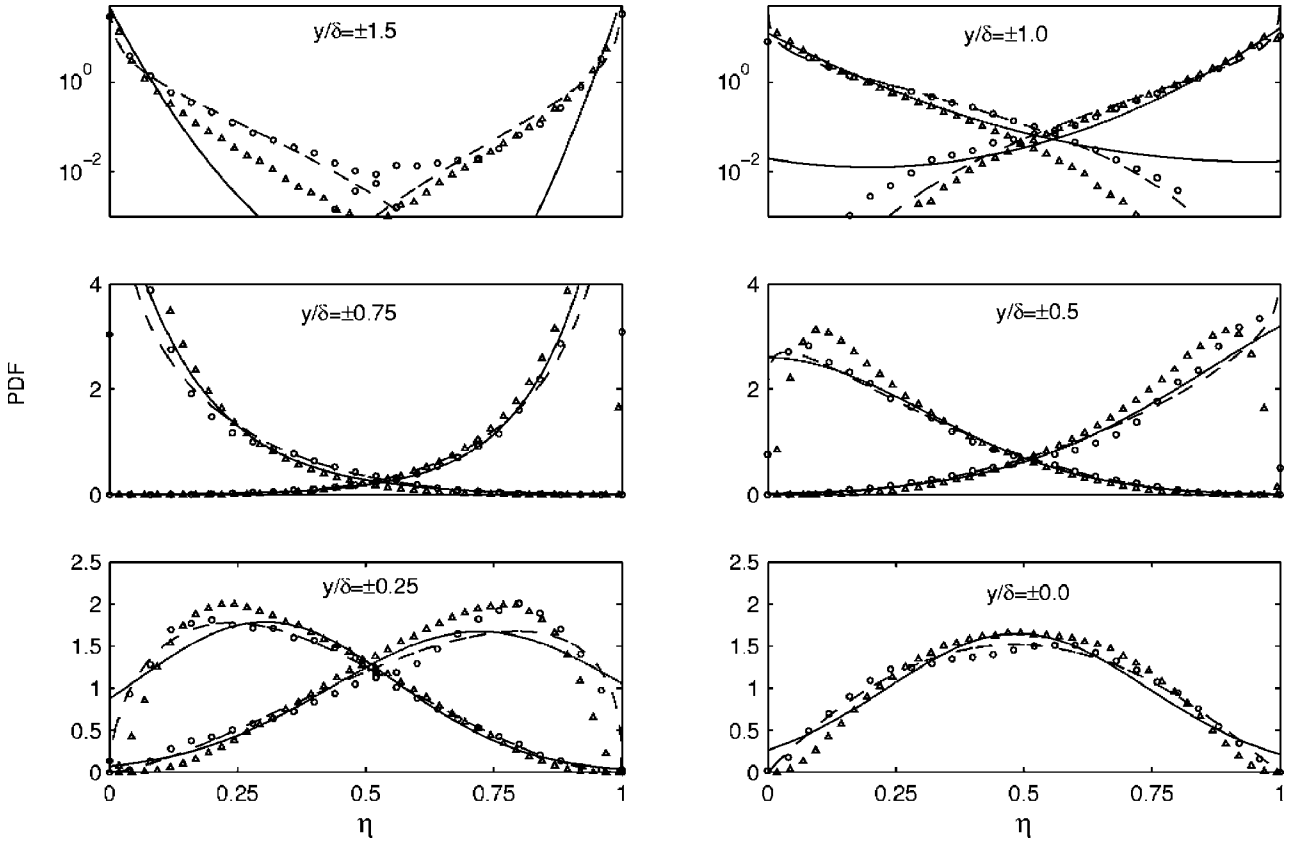

FIG. 2. Probability density of ξ at different transverse locations. DNS is represented with an ○, the β-PDF with a dashed line, the SML-PDF with a solid line. and the Lagrangian simulation with a triangle. Note that the curves for high y/δ values are plotted on a log scale.

III. SIMULATION RESULTS AND DISCUSSION

In this section we present DNS results for a variety of measures of scalar mixing. For the conditional mixing statistics, the most commonly adopted Eulerian models will be described in some detail and presented along with the results from Sawford's Lagrangian simulations using the interaction by exchange with the conditional mean (IECM) closure model . Since the latter were recently presented,[2] but without comparison to DNS data, we do not repeat the discussion of them here. Also, we note that for typical engineering problems, stochastic simulation of the JPDF equation using the IECM closure is a significantly different undertaking from simulation techniques commonly in use today, and discussion of the relative merits of each method is beyond the scope of the current paper.

A. Probability densities

Interpretation of many of the results in the following sections depend on understanding the probability density of the mixture fraction at various transverse locations in the scalar mixing layer. Therefore, we begin our discussion by considering Fig. 2 in which are shown the PDFs from the simulation together with the presumed β-PDF and the statistically most likely (SML) PDF, both calculated from the first two moments of the scalar. Also shown is the PDF from the Lagrangian simulations with the IECM closure. The β-PDF is found from[15]

$$p_\xi(\eta) = \eta^{a-1}(1-\eta)^{b-1}\frac{\Gamma(a+b)}{\Gamma(a)\Gamma(b)}, \tag{2}$$

where

$$a = \bar{\xi}\left(\frac{\bar{\xi}(1-\bar{\xi})}{\overline{\xi'^2}} - 1\right), \quad b = a\frac{1-\bar{\xi}}{\bar{\xi}} \tag{3}$$

and Γ is the gamma function. The SML-PDF is found from[16]

$$p_\xi(\eta) = \sum_{k=1}^{n} \exp(A_k \eta^{k-1}), \tag{4}$$

where the n parameters A_k are determined by making (4) satisfy the first $n-1$ scalar moments and integrate to unity. One attraction of the SML model is that it can be adapted to any number of mixture fraction moments. A review of the literature shows that the first two moments are used almost exclusively in modeling binary mixing, however, so that we do not investigate here the effect of increasing the number of parameters.

From Fig. 2, it is apparent that both the β-PDF model and the Lagrangian technique with the IECM closure predict the DNS data very well for all values of y/δ. The SML model does less well, especially far from the centerline of the layer, and overpredicts the probability density near the centerline as $\xi \to 0$ and $\xi \to 1$. It is also informative how low is the probability of a fluid parcel being transported from one

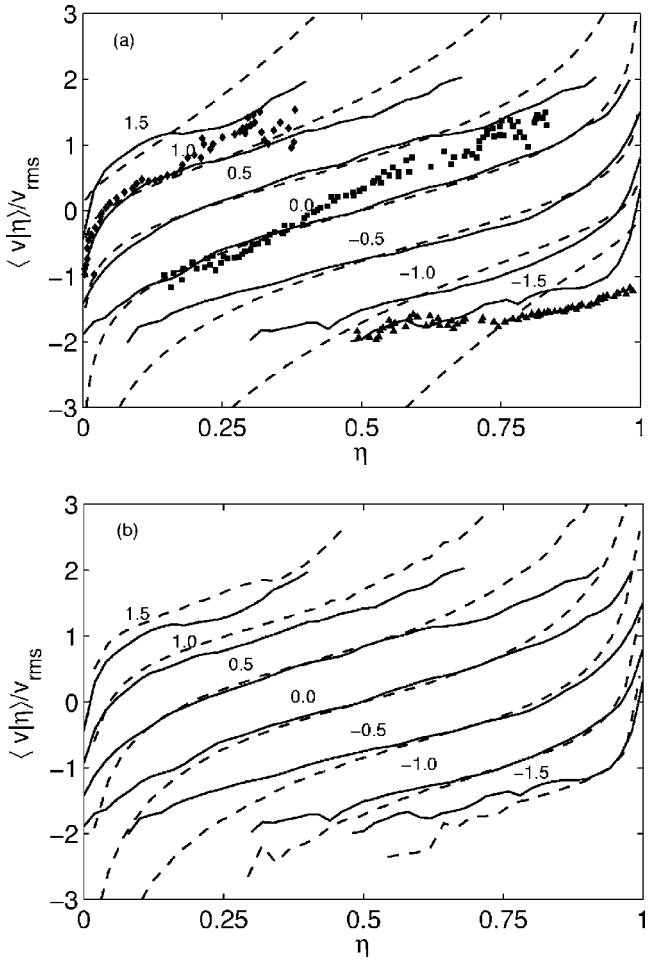

FIG. 3. The conditional mean transverse velocity at various cross-stream locations. The solid lines denote the DNS results with the numbers above each set of data indicating the y/δ value. The symbols in (a) are from Ref. 3 for $x/M=19$ and $y/\delta=-1.3$, 0.1, and 1.28. The dashed lines in (a) correspond to (6) computed with the presumed β-PDF for the same positions as the DNS. The dashed lines in (b) correspond to the Lagrangian simulation.

side of the layer to the other without mixing. For instance, considering the top left panel of Fig. 2 in which p_ξ is shown for $y/\delta=-1$, the probability density of $\xi=0.5$ occurring this far from the center is quite small.

B. Conditional mean velocity

The conditional mean transverse velocity normalized by the rms transverse velocity v_{rms}, is plotted in Fig. 3 for various values of y/δ. The results are consistent with the laboratory data from Ref. 4, which are shown in the same figure. Despite the large size of the DNS data set, there is still an unexpected lack of symmetry between $y/\delta=-1.5$ and 1.5, which is most likely a symptom of too small a sample size to yield results with high certainty at these locations. At smaller values of $|y/\delta|$, however, the curves from the DNS data are fairly smooth and show the expected symmetry. For all positions of $|y/\delta|$, the part of the conditional mean velocity that can be resolved is well described by an inverse error function. This is even more clear from Fig. 4, where the DNS data are plotted according to the model of Li and Bilger[3] described in (7).

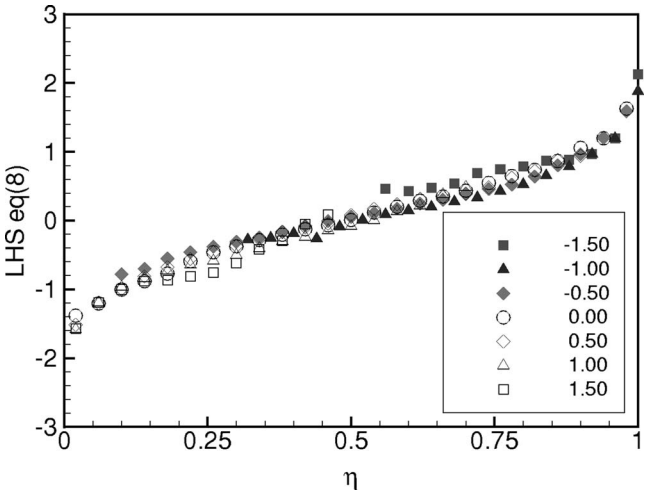

FIG. 4. The conditional mean transverse velocity at various cross-stream locations. The data have been normalized in accordance with the model of Li and Bilger.

Modeling of the conditional mean velocity is complicated by the fact that the term implies the unconditional fluxes of all the moments of any scalar. For the mixture fraction, and similarly for other passive scalars, we have the following identity:

$$\overline{\mathbf{v}\xi'^n}=\int_{\eta^-}^{\eta^+}\eta'^n\langle\mathbf{v}|\eta\rangle p_\xi(\eta)d\eta, \tag{5}$$

where the primes indicate fluctuations about the mean, n is an integer denoting the moment of the scalar fluctuations, and η^- to η^+ describes the span of the mixture fraction space. This suggests that models for the conditional velocity should be consistent with conservation of the scalar. The only model we know of for which this property is guaranteed for both passive and reactive scalars is the gradient diffusion model proposed by Pope:[11]

$$\langle v|\eta\rangle=-\frac{\kappa_T}{p_\xi}\frac{\partial p_\xi}{\partial y}, \tag{6}$$

where κ_T is the turbulent diffusion coefficient that can be computed from the DNS. Obviously, the accuracy of (6) will depend on how p_ξ is calculated, either by solving (1) or by assuming a model. For the commonly used β-PDF, discussed in Sec. III A, the predictions from (6) are compared to the DNS results in Fig. 3. The model predicts the DNS results very well where the β-PDF agrees with the DNS (cf. Fig. 2), but at low probability densities the conditional velocity diverges to $\pm\infty$. This characteristic has been previously reported in the literature[2,17] and may not be important, since the events occurring at low probability densities have little effect on overall mixing. It may also just be a feature of the β-PDF since it can be shown that a Gaussian scalar PDF gives a well behaved conditional velocity at all probability densities. The major attraction of (6) is that no other model conserves the unconditional reactive scalar when used in moment methods.[18]

One of the main advantages of the Lagrangian modeling techniques used by Sawford[2] is that convection is treated

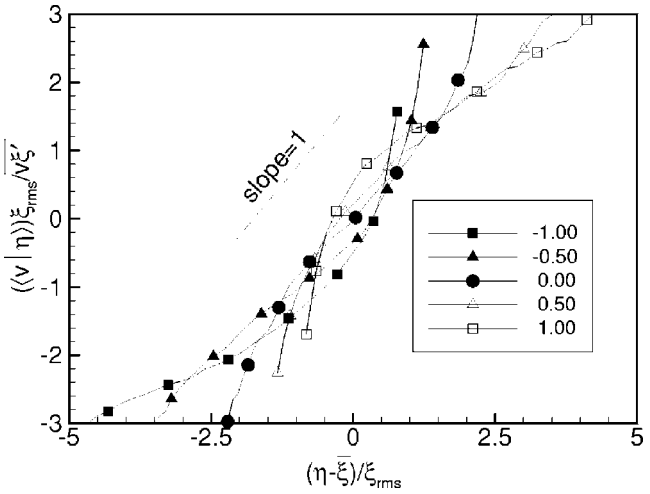

FIG. 5. The conditional mean transverse velocity at various cross-stream locations. The data have been normalized in accordance with the linear model.

exactly, without modeling assumptions. Used in conjunction with the IECM closure, it predicts conditional velocities that are in excellent agreement with the the DNS results as shown in Fig. 3(b). In fact, the Lagrangian technique yields conditional velocity profiles that are closer to the inverse error function than are the DNS results. Kuznetsov and Sabel'nikov[19] suggest that the large fast eddies required to produce very high conditional velocities might not be expected to exist in a real flow, however, so that it remains an open, and perhaps not very interesting, question as to what happens with $\langle v|\eta\rangle$ when p_ξ is very small.

Li and Bilger[3] propose a model originally developed for scalar mixing layers:

$$\langle v|\eta\rangle = \langle v|\eta=\bar{\xi}\rangle + \alpha\frac{v}{\delta}(y-y_\eta). \tag{7}$$

Here y is the location of interest, y_η is the location where the local mean mixture fraction is equal to η, and α is a constant. This equation can be rewritten as

$$(\langle v|\eta\rangle - \langle v|\eta=\bar{\xi}\rangle)/(\alpha v) - \frac{y}{\delta} = -\frac{y_\eta}{\delta}, \tag{8}$$

where the right-hand side is a function of η only. The DNS data scaled in accordance with (8), plotted in Fig. 4, collapse quite well to the inverse error function, which is consistent with the common assumption that $\xi(y)$ can be modeled well by the error function. The value $\alpha=1.3$ was chosen by using linear regression to best collapse the curves at $\eta=0.5$. Li and Bilger propose $\alpha\approx 1$. The dimensional reasoning on which (7) is based does not provide a value for α, so that the fact that we and Li and Bilger both arrive at order one values for α is encouraging.

A common modeling approach is to assume[20] a linear model that holds exactly for flows in which the JPDF is Gaussian. For the scalar mixing layer, this may be expressed

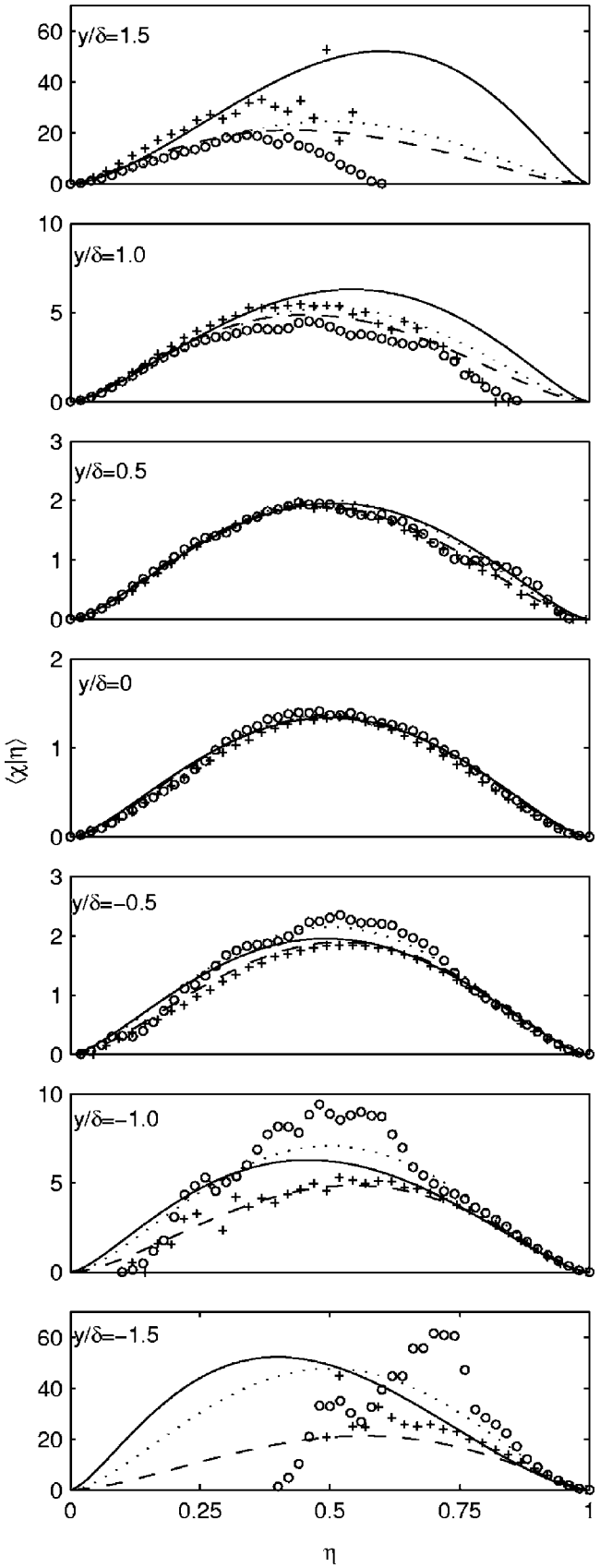

FIG. 6. The conditional scalar dissipation rate at various cross-stream locations normalized by $\bar{\chi}$. Different transverse locations are shown in each panel. Equation (12) is calculated from the β-PDF and Mortensen's full model is represented with solid lines, whereas the homogeneous part is represented with dashed lines. The counterflow model is represented with dotted lines and the Lagrangian simulation results are represented with "+". Open circles are the DNS data.

$$\langle v|\eta\rangle = \frac{\overline{v\xi'}}{\overline{\xi'^2}}(\eta - \tilde{\xi}), \tag{9}$$

where the overbar denotes the mean. It is generally recognized that this modeling approach does not account for the behavior of $\langle v|\eta\rangle$ when η is far from the local mean mixture fraction. In Fig. 5, the DNS data are plotted so as to collapse to a straight line if (9) were true. It is apparent that the model is only reasonable over a limited range of η for each y/δ location.

C. Conditional scalar dissipation rate

The conditional scalar dissipation rate (CSD) is a measure of the scalar mixing rate conditional on the value of the scalar itself and can be defined as

$$\langle \chi|\eta\rangle \equiv 2\kappa\langle \nabla\xi\cdot\nabla\xi|\eta\rangle. \tag{10}$$

The CSD and the scalar PDF are strongly coupled through (1). For homogeneous mixing, it is actually sufficient to know the PDF in order to calculate the CSD, and vice versa. The strong coupling to the PDF makes good, general models for the CSD hard to come by. For simple, binary, canonical flows, however, like the scalar mixing layer, the PDFs will be unimodal and models for the CSD can be expected to perform well.

The conditional scalar dissipation rates from the DNSs are plotted in Fig. 6 for various cross-stream locations. As with the conditional velocity, there are not enough occurrences in the DNS data of the scalar being transported across the layer without mixing for good statistics to be obtained over the whole range of η far from the centerline. For $|y/\delta| < 1.5$, the shape of the CSD appears to be quite universal, though. The universal shape is in accordance with theories of mixing taking place through diffusion in thin sheet structures, as suggested by, e.g., Buch and Dahm.[21] A universal profile is also consistent with the amplitude mapping closure of Chen *et al.*,[22] or equally the counterflow model of Peters.[23] All these theories arrive at the same expression for the CSD:

$$\langle \chi|\eta\rangle = N\overline{\chi}\exp\{-2[\mathrm{erf}^{-1}(2\eta-1)]^2\}, \tag{11}$$

where N is a normalization factor and erf^{-1} is the inverse of the error function. The fact that seemingly completely different arguments lead to the same model is strong support for the validity of (11). In all the aforementioned models, however, it is assumed that both pure fluids are present; i.e., that $\xi=0$ and $\xi=1$ exist. For large $|y/\delta|$ in the scalar mixing layer, this assumption does not hold, and it can be expected that (11) will not perform well in these regions. Equation (11) is shown as the dotted line in Fig. 6, where good agreement between the model and the DNS data can be observed for all positions where the DNS data spans the entire range of η. Equation (11) is also in close agreement with the results of the Lagrangian simulation closed with the IECM model, but for the latter, there are, as for the DNS, no results available where the probability densities of ξ are low. Note that the scaling constant N in (11) was determined by p_ξ from the DNS.

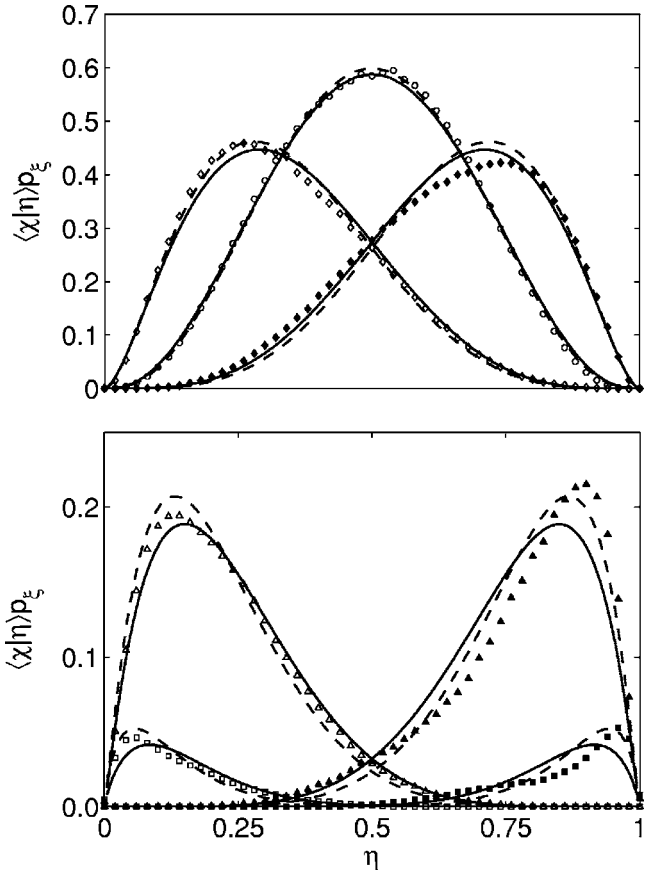

FIG. 7. The conditional scalar dissipation rate times the PDF at various cross-stream locations. The PDF is presumed with the β-PDF. Symbols are the same as in Fig. 4. The solid line represents Mortensen's full model, whereas the dashed line is the homogeneous part, corresponding to Girimaji's model.

Recently, Mortensen[18] derived an expression for the conditional scalar dissipation rate by integrating (1) and making use of the consistent transport equations for the moments. The model ensures that implementations of the classical approach to conditional moment closure[14] are self-consistent for inhomogeneous flows. Neglecting the contribution from molecular diffusion, the CSD for a two-parameter presumed PDF can be written as

$$\frac{1}{2}\langle \chi|\eta\rangle p_\xi(\eta) = \frac{\partial II(\eta)}{\partial \overline{\xi'^2}}[\overline{\chi} - 2\kappa_T(\nabla\tilde{\xi})^2] + \kappa_T \frac{\partial^2 II(\eta)}{\partial\mu_j\,\partial\mu_k}\frac{\partial\mu_j}{\partial x_i}\frac{\partial\mu_k}{\partial x_i}, \tag{12}$$

where $II(\eta)$ is the double integral over p_ξ and μ is a vector of mixture fraction moments; i.e $\mu=(\tilde{\xi},\overline{\xi'^2})$. The tensor notation implies summation. The terms involving spatial gradients of mean properties yields an inhomogeneous modification arising from combined effects of the gradient diffusion model (6) for the conditional mean velocity and the presumed form of the PDF. Equation (12) is computed with the presumed β-PDF and is plotted in Fig. 6 for comparison with (11), the Lagrangian simulation results, and the DNS data. The mean profiles required for (12) have been found by fitting a symmetric error function to the mean mixture fraction

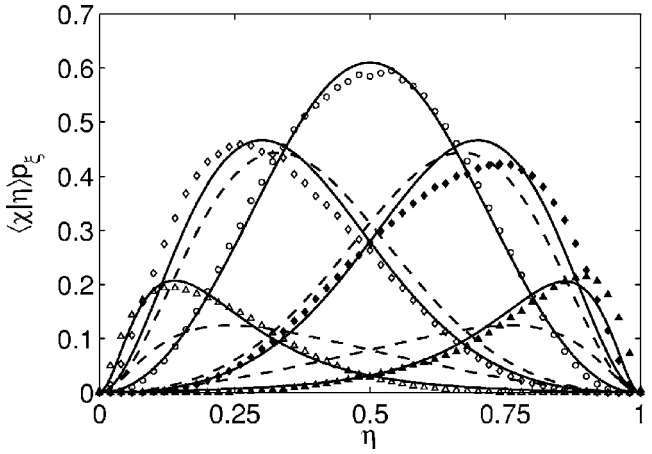

FIG. 8. The conditional scalar dissipation rate times the PDF at various cross-stream locations. The PDF is presumed with the SML-PDF. Symbols are the same as in Fig. 4. The solid line represents Mortensen's full model, whereas the dashed line is the homogeneous part.

and a Gaussian with zero mean to the variance. Hence the CSDs calculated from (12) will be symmetrical about the center of the mixing layer, even though the DNSs are slightly asymmetric.

When used with the β-PDF, the homogeneous part of (12) (the term not including spatial gradients) is equivalent to the commonly adopted model of Girimaji.[24] To investigate the effects of the inhomogeneous modifications, we plot in Fig. 6 both the full model and the homogeneous part. For small $|y/\delta|$, the inhomogeneous terms have only minor effects. Further from the centerline, though, the correction for inhomogeneity is to increase the mixing rate where there is very low probability of finding the scalar and vice versa for high probability. This trend would seem to be consistent with our physical intuition about how fluids mix. Consider the hypothetical case in which a fluid parcel with $\xi=0.8$ is advected completely across the layer to $y/\delta=1.5$. This would cause the local scalar dissipation rate to be quite high, and the CSD to be high also, which is exactly what the inhomogeneous term predicts. Unfortunately, it is not likely possible to verify this reasoning with simulation or laboratory data due to the limiting velocity of the large eddies in the flow field.[19]

In Fig. 7 we plot the CSD multiplied by p_ξ. From this figure it is evident that the differences between the model predictions from (12) and the DNS where p_ξ is low will have little effect on predictions for the overall mixing rate. When using the β-PDF, the weighted effect of including the inhomogeneous term are small, and only for $y/\delta=\pm1.5$, is it evident that including this term improves upon Girimaji's model. To see if the small improvement due to the inhomogeneous term only results when the β-PDF is used, we plot in Fig. 8 the CSD times the probability density of ξ assuming the SML-PDF. For this presumed PDF, the effect of the inhomogeneous term is to significantly increase the accuracy of the model for all positions off the centerline. This suggests that consistency between the model for the PDF and the model for the CSD will minimize the effect of errors in the PDF on predictions of overall mixing rate.

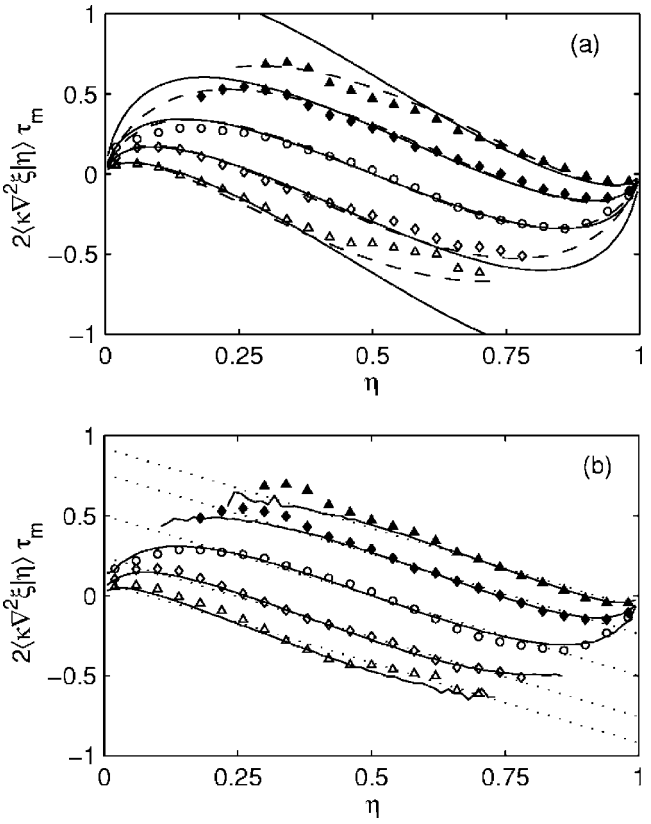

FIG. 9. The conditional scalar diffusion rate normalized by the mixing time scale, $\tau_m=\overline{\xi'^2}/\tilde{\chi}$, at various cross-stream locations. Symbols are the same as in Fig. 4. In (a), Mortensen's model is shown for both the full model (solid line) and the homogeneous part (dashed line) using the β-PDF. In (b), Sawford's Lagrangian simulation (solid lines) and the IEM model (dotted lines) are shown.

Note, finally, that even though the inhomogeneous modifications are small for the β-PDF, only the full model is completely consistent when applied with the conditional moment closure. The result of only using the homogeneous part will be a false chemistry term that may or may not be significant, depending on the flow under consideration.

Equation (12) is to be interpreted as a consequence rather than as a model derived from observations. The reason for this is that, for a presumed p_ξ, (12) provides the corresponding CSD. Thus, once a model for the scalar PDF has been chosen, the only consistent conditional scalar dissipation rate follows from (12). The one assumption being made here is that the commonly adopted gradient diffusion hypothesis for the scalar flux applies. Note that since (12) is a consequence of the presumed PDF, it is not intended as a CSD model for transported PDF methods. If used in transported PDF methods, the model would merely result in the presumed PDF. For transported PDF methods, consistency of the moments is implied through solution of (1), and only the homogeneous part of (12) should be used.

D. Conditional scalar diffusion rate

The rate of molecular mixing is usually described by the conditional scalar dissipation rate in the flamelet or conditional moment closure approaches to combustion modeling.

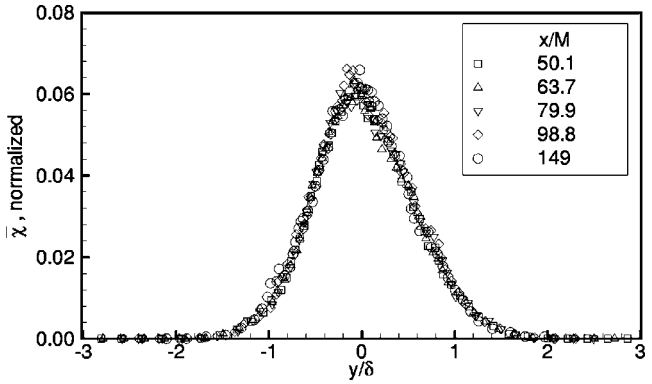

FIG. 10. Profiles of $\bar{\chi}\bar{k}/\bar{\epsilon}$.

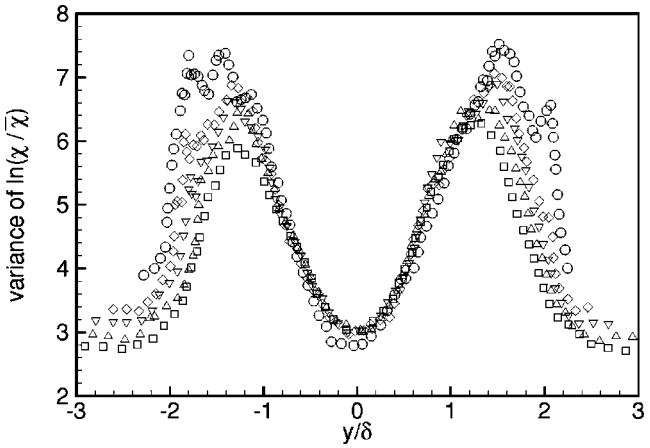

FIG. 12. Profiles of the variance of $\ln(\chi/\bar{\chi})$. Symbols are the same as in Fig. 10.

For transported PDF methods, though, the preferred term is the conditional scalar diffusion rate (also termed the Laplacian) defined as $\langle \kappa \nabla^2 \xi | \eta \rangle$. The CSD and the Laplacian contain equivalent information. The Laplacian from DNS is plotted in Fig. 9 together with the Laplacian counterpart of (12) (again using the β-PDF) for several cross-stream locations. Note that to calculate the Laplacian, it is sufficient to replace the double integral $II(\eta)$ in (12) with a single integral. Also shown in Fig. 9 is the contribution from just the homogeneous part of (12) and the results of the Lagrangian simulation. The homogeneous term apparently captures both the shape and the magnitude of the DNS profile very well, while the addition of the inhomogeneous part appears to result in less good predictions in regions where p_ξ is small. As with the CSD, however, the significance of this effect is not clear. The Lagrangian dispersion model closed with the IECM agrees very well with the DNS for all locations in scalar mixing layer.

The most commonly adopted model for the conditional diffusion is the IEM model of Villermaux and Devillon:[25]

$$\langle \kappa \nabla^2 \xi' | \eta \rangle = \frac{\bar{\chi}}{2\overline{\xi'^2}} (\bar{\xi} - \eta). \tag{13}$$

The IEM model is illustrated with the dotted lines in Fig. 9. The linearity of (13) is not reflected in the DNS, which is consistent with results reported elsewhere.[2,17] Neither is the Laplacian from DNS necessarily zero for the local mean mixture fraction, which is implied by the IEM model. The major shortcoming of the IEM model, though, is that for homogeneous turbulence it leaves the shape of the scalar PDF unchanged.[26] The popularity of the IEM model is attributed mainly to its low cost and ease of use. For inhomogeneous flows, it has also been observed that the turbulent velocity fluctuations will yield a Gaussian PDF in the absence of a molecular mixing model.[26] Hence, the shape of the Laplacian can sometimes be argued to be of lesser importance, and the IEM model can still give acceptable results.

E. Other quantities

The DNS results and various model predictions for the terms in (1) were discussed in some detail in the preceding sections because it is these terms that form the basis for many current efforts to model non-premixed turbulent combustion. A number of other quantities, however, are used either directly in, to provide justification for, or as cross-checks for, a variety of models. These quantities include the unconditionally averaged scalar dissipation rate, the fluxes of the

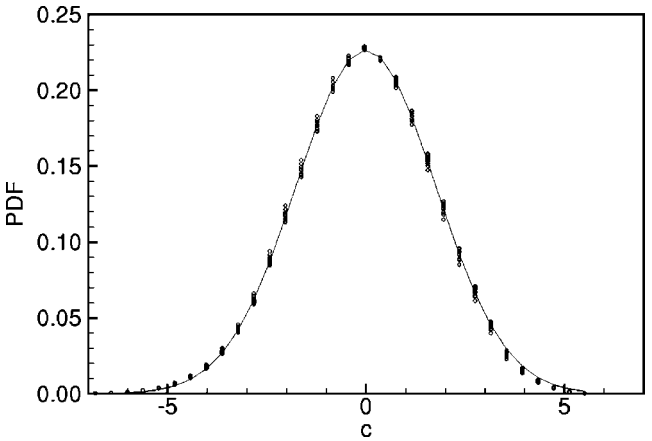

FIG. 11. Probability density of $\ln(\chi/\chi_{mp})$ with c being the probability space counterpart to χ. The symbols are from the DNS and the line is the Gaussian function.

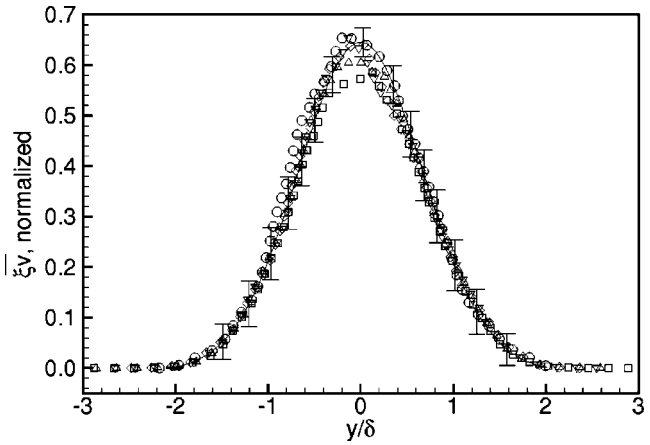

FIG. 13. Profiles of the scalar flux normalized by I_{max} and v_{rms}. Symbols are the same as in Fig. 10. The line and error bars represent the data from Ref. 8.

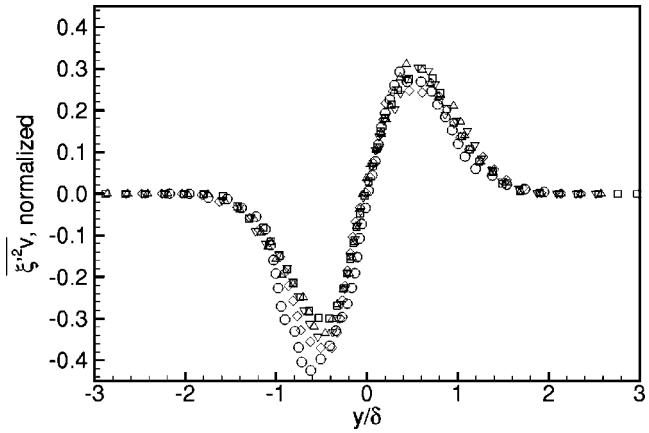

FIG. 14. Profiles of the flux of the scalar variance normalized by $I_{\max}^2$ and $v_{\rm rms}$. Symbols are the same as in Fig. 10.

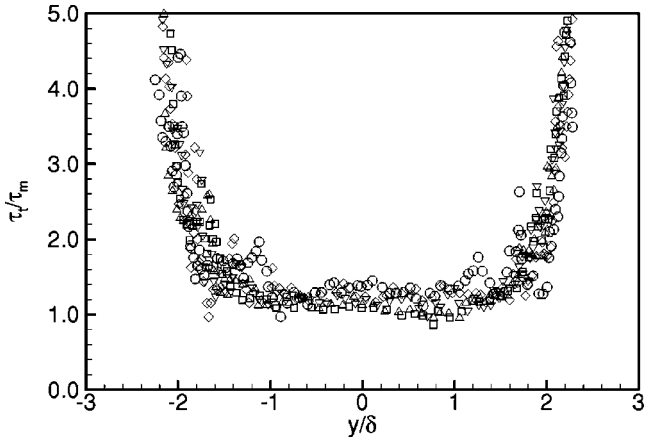

FIG. 16. Ratio of the turbulent time scale to the mixing time scale. Symbols are the same as in Fig. 10.

scalar and its variance, the ratio of the mixing and turbulent time scales, and the turbulent diffusivity. A comprehensive review of models for each of these statistics is beyond the scope of this paper; the DNS results are presented for reference with limited discussion.

1. Scalar dissipation rate

Discussed above is the scalar dissipation rate conditionally averaged on the value of the scalar. It is also useful, however, to understand how $\bar{\chi}$ varies in space, and to be able to predict the behavior of the probability density of χ. The normalized profile of $\bar{\chi}$ is plotted in Fig. 10. The data collapse very well to a common profile.

The probability density of χ is often taken to be log normal. From Fig. 11, it is apparent that the DNS data strongly support this assumption. In the figure, the PDF of $\ln(\chi/\chi_{\rm mp})$ is plotted, where $\chi_{\rm mp}$ is the most probable value. The symbols on the plot represent the DNS data at five streamwise locations between $x/M=50.1$ to $x/M=149$ and 15 transverse locations from $y/\delta=-2$ to 2, and the line is the best fit Gaussian curve. It is interesting to note that even at $y/\delta=\pm 2$, where many statistics show the effects of intermittency, the PDF of χ is almost exactly log normal. A quantity related to the PDF of $\ln(\chi/\chi_{\rm mp})$ is the profile of the variance of $\ln(\chi/\bar{\chi})$, which is shown in Fig. 10.

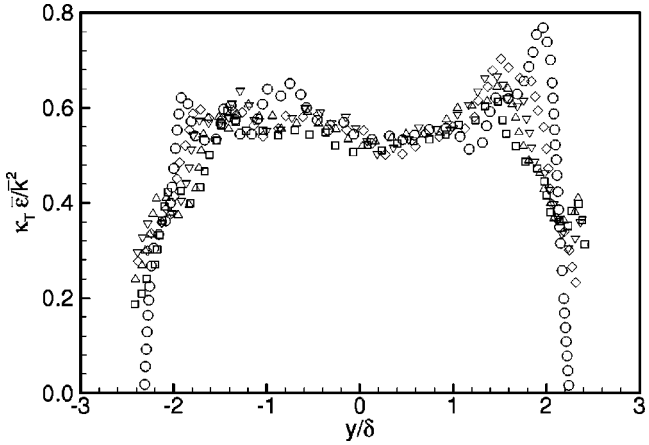

FIG. 15. Profiles of the normalized turbulent diffusivity, $\kappa_T/u_{\rm rms}\delta$. Symbols are the same as in Fig. 10.

2. Fluxes

The fluxes of moments of the scalar are basic measures of the rate of large scale mixing, or stirring, of the scalar field. They are related to the conditional velocity through (5) and thus are used in modeling $\langle v|\eta\rangle$. For the scalar mixing layer at high Peclet number, the profiles of the fluxes can be expected to have a universal shape,[27] and thus can be used as a measure of how close an experimental or simulated flow is to self-similarity.[8] Here we consider the fluxes of just the first two moments, which are shown in Figs. 13 and 14. For consistency with Ref. 8, the peak of the scalar fluctuation intensity ($I_{\max}$) and the rms of the transverse velocity fluctuations are used to normalize the data, although nearly perfect collapse of both sets of profiles can be obtained by using the scaling consistent with self-similarity assuming power law behavior for the length and velocity scales. The scalar flux profiles agree very well with experimental results of Ma and Warhaft,[8] which are also shown in the figure.

3. Turbulent diffusivity

A turbulent diffusivity can be defined in terms of (6) or, equivalently, $\kappa_T \equiv \overline{vz}/\partial\xi/\partial y$. Similarity analysis leads us to expect $\kappa_T\bar{\epsilon}/\bar{k}^2$ to be a function of y/δ only, as is shown to be the case in Fig. 15. The scaled turbulent diffusivity is nearly constant at about 0.55 in the layer and tends to increase slightly in the intermittent regions at the edges of the layer. The ratio of the turbulent and molecular diffusivities, κ_T/κ, ranges from 73 at $x/M=50.1$ to 47 at $x/M=149$, which indicates that molecular effects are quite small throughout the simulation, but do become more pronounced as the velocity field decays.

4. Ratio of time scales

For many turbulent flows, a lot is known about how to model the turbulent time scale, $\tau_t=\bar{k}/\bar{\epsilon}$, where $\bar{k}$ and $\bar{\epsilon}$ are the Reynolds averaged turbulence kinetic energy and its dissipa-

tion rate, respectively. The analogous time scale for mixing is $\tau_m = \overline{\xi'^2}/\bar{\chi}$ and the ratio of the time scales can be defined as $r = \tau_t/\tau_m$. In grid turbulence, the turbulence kinetic energy and the scalar variance decay according to the power laws

$$\overline{\xi'^2} = A\frac{(x - x_{0,\xi})^{-m}}{M},$$

$$\bar{k} = B\frac{(x - x_0)^{-n}}{M},$$

where x_0 and $x_{0,\xi}$ are the virtual origins of the velocity and scalar fields, respectively. Thus, for grid turbulence, $r = m/n$, and values in the range 0.6–2.5 have been measured in the laboratory.[28,29] Durbin[30] explained the variation between the different laboratory experiments by showing that r will depend on the initial ratio of the characteristic length scales of the turbulence and scalar.

The perfectly self-similar scalar mixing layer is a special case in which $x_0 = x_{0,\xi}$ and $m = n$, so that $r = 1$. The DNS results are plotted in Fig. 16 as a function of y/δ for several downstream locations. For a given downstream location, the ratio is nearly constant across the layer and then increases rapidly in the intermittent region at the edge of the layer. At the center of the layer, r increases from 1.1 at $x/M = 50.1$ to 1.3 at $x/M = 149$. The deviation from unity of the time scale ratio is due to the departure from self-similarity of the simulated flow, which becomes more pronounced as the flow decays and the effects of moderate Peclet and Reynolds numbers become more pronounced. Note that the Schmidt number is 0.7.

IV. CONCLUSIONS

As modeling methods for turbulent reacting flows develop, there continues to be a demand for new data against which to compare model results, even for simple flows that have been previously studied extensively. One technique to meet this demand is direct numerical simulations since, once validated, the resulting data sets can be mined for arbitrary quantities as they become of interest to modelers. In this paper, we present conditional mixing statistics from high resolution, direct numerical simulations of a very nearly canonical scalar mixing layer. The results are presented in a form useful for testing transported PDF, conditional moment closure, and other models. Based on the results reported here and in Ref. 4, we conclude that the simulation data set provides an excellent description of a canonical scalar mixing layer, as a function of three spatial dimensions and time, for use in developing and verifying mixing models. The data set is available by contacting the first author.

In addition to providing a comprehensive set of mixing statistics for the scalar mixing layer, a model for the conditional scalar dissipation rate, recently introduced by Mortensen,[18] is evaluated for the scalar mixing layer. The model extends that of Girimaji[24] to ensure that implementations of the classical approach to conditional moment closure are self-consistent for inhomogeneous flows. The new model is not an improvement over Girimaji's for the current simple flow when the PDF of the scalar is well modeled, but the internally self-consistent character of Mortensen's model does result in improved prediction of the CSD multiplied by p_ξ when p_ξ is not well modeled.

Finally, results of a Lagrangian simulation[2] of the joint velocity-scalar PDF closed with the interaction by exchange with the conditional mean (IECM) model are presented. In part because the convection term is computed exactly in the Lagrangian approach, the IECM closure yields very good predictions for all of the conditional statistics and the probability density of ξ.

ACKNOWLEDGMENTS

The authors thank Professor B. L. Sawford for providing us with the Lagrangian simulation results. We also thank Professor Sawford and Professor R. W. Bilger for their feedback on early drafts of this paper. S.M.d.B.K. was supported by the National Science Foundation (Grant No. CTS9810103) and the Air Force Office of Scientific Research (Grant No. F49620-97-1-0092). M.M. was sponsored by the Center for Chemical Process Design and Control through the Swedish Foundation for Strategic Research. High-performance computing resources for this research were provided by the Arctic Region Supercomputing Center.

[1] R. W. Bilger, "Some aspects of scalar dissipation," Flow, Turbul. Combust. **72**, 93 (2004).
[2] B. L. Sawford, "Conditional scalar mixing statistics in homogenous isotropic turbulence," New J. Phys. **6**, 1 (2004).
[3] J. D. Li and R. W. Bilger, "A simple theory of conditional mean velocity in turbulent scalar-mixing layer," Phys. Fluids **6**, 605 (1994).
[4] S. M. de Bruyn Kops and J. J. Riley, "Re-examining the thermal mixing layer with numerical simulations," Phys. Fluids **12**, 185 (2000).
[5] W. E. Watt and W. D. Baines, "The turbulent temperature mixing layer," J. Hydraul. Res. **11**, 158 (1973).
[6] J. C. LaRue and P. A. Libby, "Thermal mixing layer downstream of half-heated turbulence grid," Phys. Fluids **24**, 597 (1981).
[7] J. C. LaRue, P. A. Libby, and D. V. R. Seshadri, "Further results on the thermal mixing layer downstream of a turbulence grid," Phys. Fluids **24**, 1927 (1981).
[8] B.-K. Ma and Z. Warhaft, "Some aspects of the thermal mixing layer in grid turbulence," Phys. Fluids **29**, 3114 (1986).
[9] J. L. Lumley, "Evolution of non-self-preserving thermal mixing layer," Phys. Fluids **29**, 3976 (1986).
[10] R. W. Bilger, L. R. Saetran, and L. V. Krishnamoorthy, "Reaction in a scalar mixing layer," J. Fluid Mech. **233**, 211 (1991).
[11] S. Pope, "PDF methods for turbulent reactive flows," Prog. Energy Combust. Sci. **11**, 119 (1985).
[12] E. E. O'Brien, in *Topics in Applied Physics*, edited by P. A. Libby and F. A. Williams (Springer, Berlin, 1980).
[13] S. M. de Bruyn Kops and J. J. Riley, "Direct numerical simulation of laboratory experiments in isotropic turbulence," Phys. Fluids **10**, 2125 (1998).
[14] R. W. Bilger, "Conditional moment closure for turbulent reacting flow," Phys. Fluids A **5**, 436 (1993).
[15] R. W. Bilger, in *Topics in Applied Physics Number 44: Turbulent Reacting Flows*, edited by P. A. Libby and F. A. Williams (Springer, New York, 1980), Chap. 3, pp. 65-113.
[16] S. B. Pope, in *Turbulent Shear Flows 2* (Springer-Verlag, Berlin, 1980), pp. 7–17.
[17] G. Brethouwer and F. T. M. Nieuwstadt, "DNS of mixing and reaction of two species in a turbulent channel flow: A validation of the conditional moment closure," Flow, Turbul. Combust. **66**, 209 (2001).
[18] M. Mortensen, "Consistent modeling of scalar mixing for presumed multiple parameter probability density functions," Phys. Fluids **17**, 018106 (2005).
[19] V. R. Kuznetsov and V. A. Sabel'nikov, *Turbulence and Combustion* (Hemisphere, New York, 1990).

[20]A. Yu. Klimenko and R. W. Bilger, "Conditional moment closure for turbulent combustion," Prog. Energy Combust. Sci. **25**, 595 (1999).
[21]K. A. Buch and W. J. A. Dahm, "Experimental-study of the fine-scale structure of conserved scalar mixing in turbulent shear flows. Part I: Sc $\gg$1," J. Fluid Mech. **317**, 21 (1996).
[22]H. Chen, S. Chen, and R. H. Kraichnan, "Probability distribution of a stochastically advected scalar field," Phys. Rev. Lett. **63**, 2657 (1989).
[23]N. Peters, "Laminar diffusion flamelet models in non-premixed turbulent combustion," Prog. Energy Combust. Sci. **10**, 319 (1984).
[24]S. S. Girimaji, "On the modeling of scalar diffusion in isotropic turbulence," Phys. Fluids A **4**, 2529 (1992).
[25]J. Villermaux and J. C. Devillon, in *2nd Int. Symp. Chem. React. Engng. B* (Elsevier, New York, 1972).
[26]R. O. Fox, *Computational Models for Turbulent Reacting Flows* (Cambridge University Press, Cambridge, UK, 2003), pp. 274–275.
[27]P. A. Libby, "Diffusion of heat downstream of a turbulence grid," Acta Astronaut. **2**, 867 (1975).
[28]K. R. Sreenivasan, S. Tavoularis, R. Henry, and S. Corrsin, "Temperature fluctuations and scales in grid generated turbulence," J. Fluid Mech. **100**, 597 (1980).
[29]Z. Warhaft and J. L. Lumley, "An experimental study of the decay of temperature fluctuations in grid-generated turbulence," J. Fluid Mech. **88**, 659 (1978).
[30]P. A. Durbin, "Analysis of the decay of temperature fluctuations in isotropic turbulence," Phys. Fluids **25**, 1328 (1982).